

CHAPTER 2

Sinusoidal Approximations

In this chapter, the properties of the series, parallel, and other resonant converters are investigated using the sinusoidal approximation. Harmonics of the switching frequency are neglected, and the tank waveforms are assumed to be purely sinusoidal. This allows simple equivalent circuits to be derived for the bridge inverter, tank, rectifier, and output filter portions of the converter, whose operation can be understood and solved using standard linear ac analysis. This intuitive approach is quite accurate for operation in the continuous conduction mode with a high-Q response, but becomes less accurate when the tank is operated with a low Q-factor or for operation in or near the discontinuous conduction mode.

The important result of this approach is that the dc voltage conversion ratio of a continuous conduction mode resonant converter is given approximately by the ac transfer function of the tank circuit, evaluated at the switching frequency. The tank is loaded by the effective output resistance, nearly equal to the output voltage divided by the output current. It is thus quite easy to determine how the tank components and circuit connections affect the converter behavior. The influence of tank component losses, transformer nonidealities, etc., on the output voltage and converter efficiency can also be found.

It is found that the series resonant converter operates with a step-down voltage conversion ratio. With a 1:1 transformer turns ratio, the dc output voltage is ideally equal to the dc input voltage when the transistor switching frequency is equal to the tank resonant frequency. The output voltage is reduced as the switching frequency is increased or decreased away from resonance. On the other hand, the parallel resonant converter is capable of both step-up and step-down of voltage levels, depending on the switching frequency and the effective tank Q-factor.

Switching loss mechanisms are also considered in this chapter. “Zero voltage switching” is a property that can be obtained in resonant converters whenever the tank presents a lagging (inductive) load to the switch network. This occurs for operation above resonance in the series

resonant converter, and it can lead to elimination of the switching loss which arises from the switch output capacitances. Likewise, “zero current switching” can be obtained when the tank presents a leading (capacitive) load to the switch network, as in the series resonant converter operation below resonance. This property allows natural commutation of thyristors, and elimination of switching loss mechanisms associated with package and other parasitic inductances.

2.1. First Order Network Models

Consider the class of resonant converters which contain a controlled switch network N_S and drive a linear resonant tank network N_T . The latter in turn is connected to an uncontrolled rectifier N_R , filter N_F and load R , which is illustrated in Fig. 2.1. Many well-known converters can be represented in this form, including the series, parallel, LCC, et al.

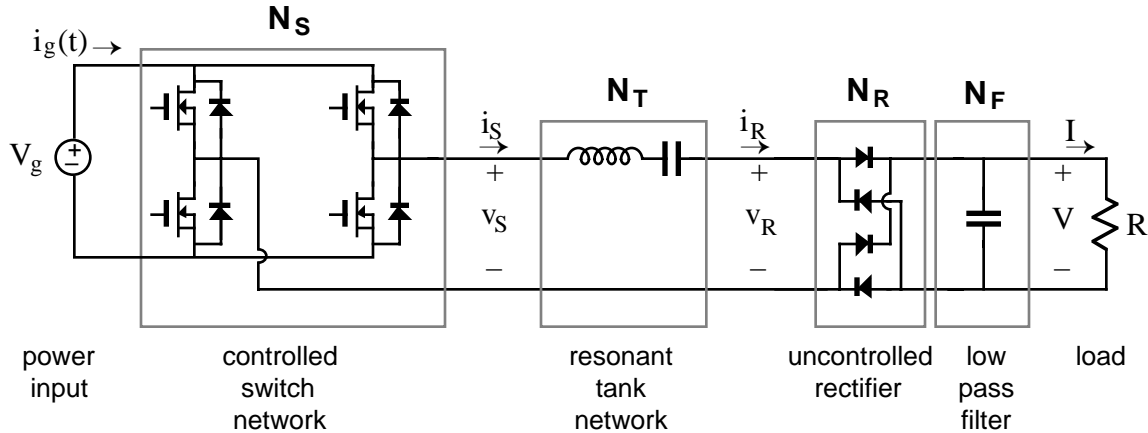


Fig. 2.1. A class of resonant converters which consist of cascaded switch, tank, rectifier, and filter networks. A series resonant converter example is shown.

In the most common modes of operation, the controlled switch network produces a square wave voltage output $v_S(t)$ whose frequency f_S is close to the tank network resonant frequency f_0 . In response, the tank network rings with approximately sinusoidal waveforms of frequency f_S . The tank output waveform v_R or i_R is then rectified by network N_R and filtered by network N_F , to produce the dc load voltage V and current I . By changing the switching frequency f_S (closer to or farther from resonance f_0), the magnitude of the tank ringing response can be modified, and hence the dc output voltage can be controlled.

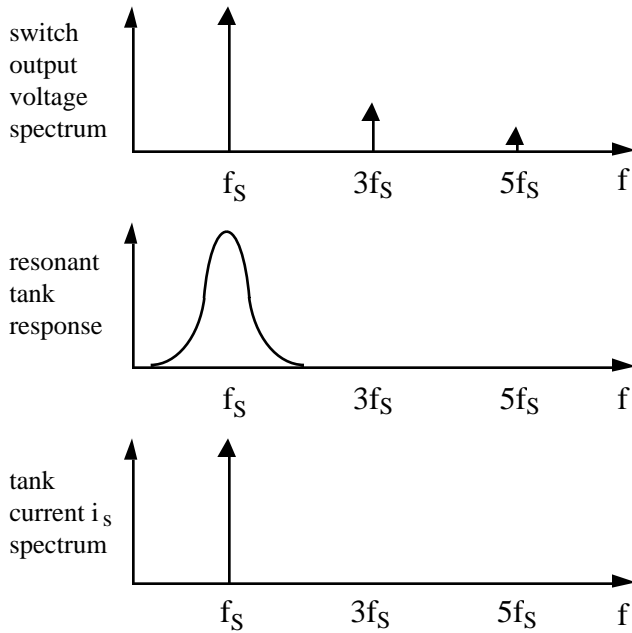


Fig. 2.2. The tank responds primarily to the fundamental component of the applied waveforms.

In the case where the resonant tank responds primarily to the fundamental component f_s of the switch waveform $v_S(t)$, and has negligible response at the harmonic frequencies nf_s , $n = 3, 5, 7, \dots$, then the tank waveforms are well approximated by their fundamental components. As shown in Fig. 2.2, this is indeed the case when the tank network contains a high-Q resonance at or near the switching frequency, and a low-pass characteristic at higher frequencies. Hence, let us neglect harmonics, and compute the relationships between the fundamental components of the tank terminal waveforms $v_S(t)$, $i_S(t)$, $i_R(t)$, and $v_R(t)$, and the

converter dc terminal quantities V_g , V , and I .

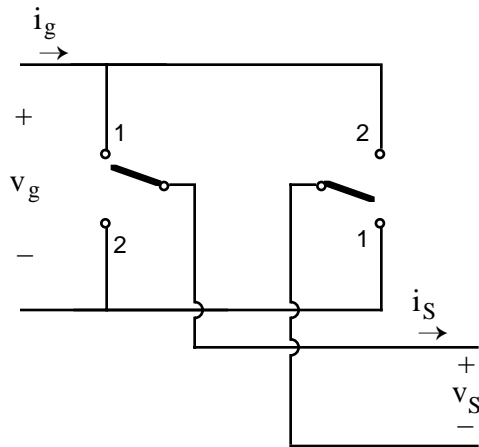


Fig. 2.3. An ideal switch network.

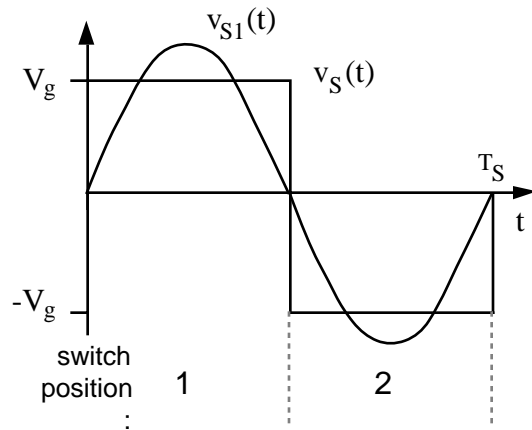


Fig. 2.4. Controlled switch network output voltage $v_S(t)$ and its fundamental component $v_{S1}(t)$.

Controlled Switch Network

If the switch of Fig. 2.3 is controlled to produce a square wave of frequency f_s as in Fig. 2.4, then its output voltage waveform $v_S(t)$ can be expressed in the Fourier series

$$v_S(t) = \frac{4 V_g}{\pi} \sum_{n=1,3,5,\dots} \frac{1}{n} \sin(2n\pi f_s t) \quad (2-1)$$

The fundamental component is

$$v_{S1}(t) = \frac{4 V_g}{\pi} \sin(2\pi f_S t) \quad (2-2)$$

which has a peak amplitude of $(4/\pi)$ times the dc input voltage V_g , and is in phase with the original square wave $v_S(t)$. Hence, the switch network output terminal is modeled as a sinusoidal voltage generator, $v_{S1}(t)$.

It is interesting to model the converter dc input. This requires computation of the dc component I_g of the switch input current $i_g(t)$. The switch input current $i_g(t)$ is equal to the output current $i_S(t)$ when the switches are in position 1, and its inverse $-i_S(t)$ when the switches are in position 2. Under the conditions described above, the tank rings sinusoidally and $i_S(t)$ is well approximated by a sinusoid of some peak amplitude I_{S1} and phase ϕ_S :

$$i_S(t) \cong I_{S1} \sin(2\pi f_S t - \phi_S) \quad (2-3)$$

The input current waveform is shown in Fig. 2.5.

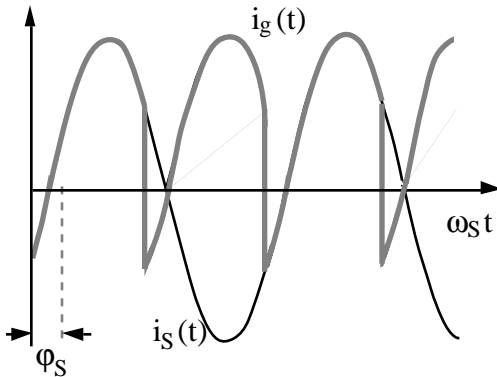


Fig. 2.5. Switch terminal current waveforms $i_g(t)$ and $i_S(t)$.

The dc component, or average value, of the input current can be found by averaging $i_g(t)$ over one half switching period:

$$\begin{aligned} \langle i_g \rangle &= \frac{2}{T_S} \int_0^{T_S/2} i_g(t) dt \\ &\cong \frac{2}{T_S} \int_0^{T_S/2} I_{S1} \sin(2\pi f_S t - \phi_S) dt \\ &= \frac{2}{\pi} I_{S1} \cos \phi_S \end{aligned} \quad (2-4)$$

Thus, the dc component of the converter input current depends directly on the peak amplitude of the tank input current I_{S1} and on the cosine of its phase shift ϕ_S .

An equivalent circuit for the switch is given in Fig. 2.6. This circuit models the basic energy conversion properties of the switch: the dc power supplied by the voltage source V_g is converted into ac power at the switch output. Note that the dc power at the source is V_g times the dc component of $i_g(t)$, and the ac power at the switch is the average of $v_S(t)$ times $i_S(t)$. Furthermore, if the harmonics of $v_S(t)$ are negligible, then the switch output voltage can be represented by its fundamental, a sinusoid $v_{S1}(t)$ of peak amplitude $4V_g/\pi$.

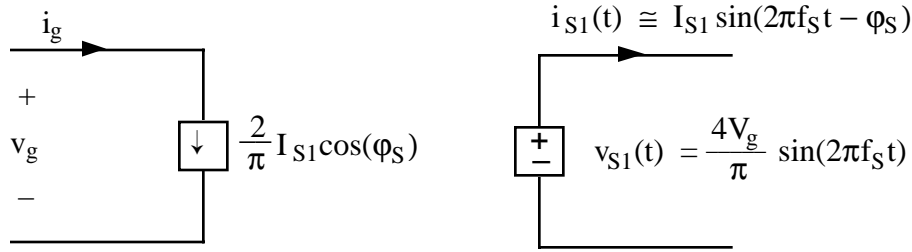


Fig. 2.6. An equivalent circuit for the switch network which models the fundamental component of the output voltage waveform and the dc component of the input current waveform.

Uncontrolled rectifier with capacitive filter network

In the series resonant converter, the output rectifier is driven by the (nearly sinusoidal) tank output current $i_R(t)$ and a large capacitor C_F is placed at the dc output, so that the output voltage V contains negligible harmonics of the switching frequency f_S , as shown in Fig. 2.8. The diode rectifiers switch when $i_R(t)$ passes through zero, as shown in Fig. 2.7, and the rectifier input voltage $v_R(t)$ is essentially a square wave, equal to $+V$ when $i_R(t)$ is positive and $-V$ when $i_R(t)$ is negative. Note that $v_R(t)$ is in phase with $i_R(t)$.

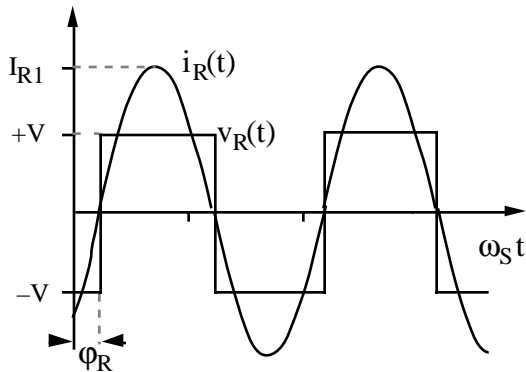


Fig. 2.7 Rectifier input waveforms $i_R(t)$ and $v_R(t)$.

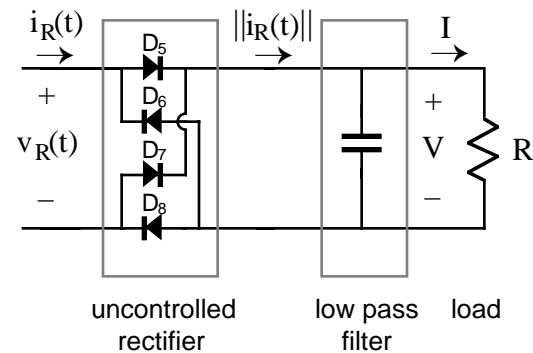


Fig 2.8 Uncontrolled rectifier with capacitive filter network, as in the series resonant converter. The diodes switch when $i_R(t)$ passes through zero.

If the tank output current $i_R(t)$ is a sinusoid with peak amplitude I_{R1} and phase shift φ_R :

$$i_R(t) = I_{R1} \sin(2\pi f_S t - \varphi_R) \quad (2-5)$$

then the rectifier input voltage may be expressed in the Fourier series

$$v_R(t) = \frac{4V}{\pi} \sum_{n=1,3,5,\dots} \frac{1}{n} \sin(2\pi n f_S t - \varphi_R) \quad (2-6)$$

where φ_R is the phase shift of $i_R(t)$. This voltage waveform is impressed on the output terminal of the resonant tank network. Again, if the tank network responds primarily to the fundamental component of f_S of $v_R(t)$, and has negligible response at the harmonic frequencies $n f_S$, $n =$

3,5,7..., then the harmonics of $v_R(t)$ can be ignored. $v_R(t)$ is then well approximated by its fundamental component $v_{R1}(t)$:

$$v_{R1}(t) = \frac{4V}{\pi} \sin(2\pi f_{st} - \phi_R) \quad (2-7)$$

The fundamental voltage component $v_{R1}(t)$ has a peak value of $(4/\pi)$ times the dc output voltage V , and it is in phase with the current $i_R(t)$.

The rectified tank output current, $|i_R(t)|$, is filtered by capacitor C_F . Since no dc current can pass through C_F , the dc component of $|i_R(t)|$ must be equal to the steady-state load current I . Equating dc components yields:

$$\begin{aligned} I &= \frac{2}{T_S} \int_0^{T_S/2} I_{R1} |\sin(2\pi f_{st} - \phi_R)| dt \\ &= \frac{2}{\pi} I_{R1} \end{aligned} \quad (2-8)$$

Therefore, the load current and the tank output current amplitudes are directly related in steady-state.

Since $v_{R1}(t)$, the fundamental component of $v_R(t)$, is in phase with $i_R(t)$, the rectifier presents an effective resistive load R_e to the tank circuit. The value of R_e is equal to the ratio of $v_{R1}(t)$ to $i_R(t)$. Division of Eq. (2-7) by Eq. (2-5), and elimination of I_{R1} using Eq. (2-8) yields

$$R_e = \frac{v_{R1}(t)}{i_R(t)} = \frac{8}{\pi^2} \frac{V}{I} \quad (2-9)$$

With a resistive load, $R = V/I$, this equation reduces to

$$R_e = \frac{8}{\pi^2} R = 0.8106 R \quad (2-10)$$

Thus, the tank network is damped by an effective load resistance R_e equal to 81% of the actual load resistance R . An equivalent circuit is given in Fig. 2.9.

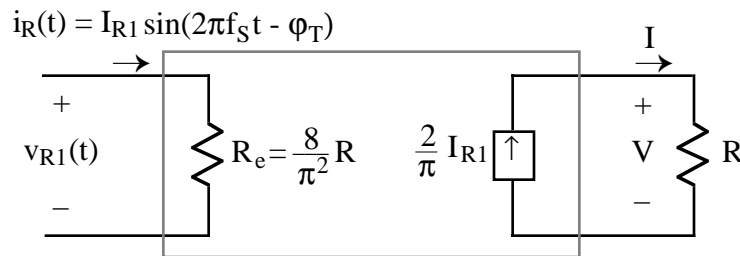
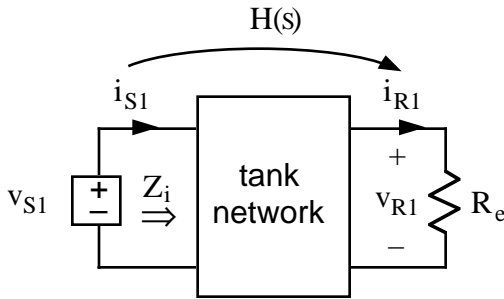


Fig. 2.9. An equivalent circuit for the uncontrolled rectifier with capacitive filter network, which models the fundamental components of the tank output waveforms $i_R(t)$ and $v_{R1}(t)$, and the dc components of the load waveforms I and V . The rectifier presents an effective resistive load R_e to the tank network.

Resonant tank network

We have postulated that the effects of harmonics can be neglected, and we have consequently shown that the bridge behaves like a fundamental voltage source $v_{S1}(t)$ and that the rectifier behaves like a resistor of value R_e . We can now solve the resonant tank network by standard linear analysis.



As shown in Fig. 2-10, the tank circuit is a linear network with the voltage transfer function:

$$\frac{v_{R1}(s)}{v_{S1}(s)} = H(s) \tag{2-11}$$

Fig. 2.10. The linear tank network, excited by an effective sinusoidal input source and driving an effective resistive load.

Hence, the ratio of the peak magnitudes of $v_{R1}(t)$ and $v_{S1}(t)$ is given by:

$$\frac{\text{peak magnitude of } v_{R1}(t)}{\text{peak magnitude of } v_{S1}(t)} = \| H(s) \|_{s=j2\pi f_s} \tag{2-12}$$

In addition, i_R is given by:

$$i_R(s) = \frac{v_{R1}(s)}{R_e} = \frac{H(s)}{R_e} v_{S1}(s) \tag{2-13}$$

So the peak magnitude of i_R is:

$$I_{R1} = \frac{\| H(s) \|_{s=j2\pi f_s}}{R_e} \cdot (\text{peak magnitude of } v_{S1}(t)) \tag{2-14}$$

Solution of converter voltage conversion ratio V/V_g

An equivalent circuit of a complete resonant converter is depicted in Fig. 2.11. The complete voltage conversion ratio of the resonant converter can now be found:

$$\frac{V}{V_g} = \underbrace{(R)}_{\left(\frac{V}{I}\right)} \cdot \underbrace{\left(\frac{2}{\pi}\right)}_{\left(\frac{I}{\|i_R\|}\right)} \cdot \underbrace{\left(\frac{1}{R_e}\right)}_{\left(\frac{\|i_R\|}{\|v_{R1}\|}\right)} \cdot \underbrace{\left(\|H_e(s)\|_{s=j2\pi f_s}\right)}_{\left(\frac{\|v_{R1}\|}{\|v_{S1}\|}\right)} \cdot \underbrace{\left(\frac{4}{\pi}\right)}_{\left(\frac{\|v_{S1}\|}{V_g}\right)} \tag{2-15}$$

Simplification by use of Eq. (2-10) yields the final result:

$$\frac{V}{V_g} = \left\| \left\| H(s) \right\| \right\|_{s=j 2\pi f_s} \quad (2-16)$$

Eq. (2-16) is the desired result. It states that the dc conversion ratio of the resonant converter is approximately the same as the ac transfer function of the resonant tank circuit, evaluated at the switching frequency f_s . This intuitive result can be applied to converters with many different types of tank circuits. However, it should be re-emphasized that Eq. (2-16) is valid only if the response of the tank circuit to the harmonics of $v_S(t)$ is negligible compared to the fundamental response, an assumption which is not always valid. In addition, we have assumed that the switch network is controlled to produce a square wave and that the rectifier network drives a capacitive-type network. Finally, the transfer function $H(s)$ is evaluated assuming that the load, R_e , is effectively resistive, and it is given by Eq. (2-10).

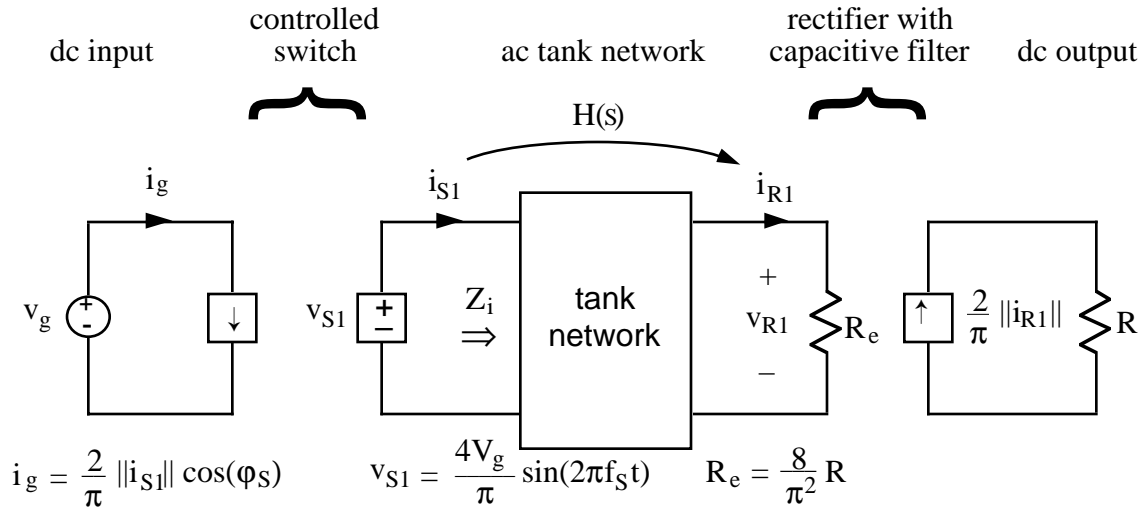


Fig. 2.11. Steady-state equivalent circuit which models the dc and fundamental components of resonant converter waveforms.

Converter efficiency

The effects of tank component losses can also be easily estimated using the model of Fig. 2.11. The converter input power is

$$P_{in} = V_g I_g = V_g \frac{2}{\pi} ||i_S|| \cos \phi_S \quad (2-17)$$

Note that $||i_S|| \cos \phi_S$ is equal to the real part of $i_S(s)$. In addition, $i_S(s)$ is equal to the switch output voltage $v_{S1}(s)$ divided by the tank input impedance $Z_i(s)$:

$$i_S(s) = \frac{v_{S1}(s)}{Z_i(s)} = Y_i(s) v_{S1}(s) \quad (2-18)$$

Hence, the real part of $i_S(s)$ is:

$$\text{Real}(i_S(s)) = \|v_{S1}(s)\| \text{Real}(Y_i(s)) = \frac{4V_g}{\pi} \cdot \text{Real}(Y_i(s)) \quad (2-19)$$

and the input power is:

$$P_{in} = \frac{8}{\pi^2} V_g^2 \text{Real}(Y_i(s)) \quad (2-20)$$

The converter output power is:

$$P_{out} = IV = \frac{\|v_{R1}\|^2}{2 R_e} \quad (2-21)$$

But $v_{R1}(s) = v_{S1}(s) H(s)$, and hence $\|v_{R1}\|^2 = \|v_{S1}(s)\|^2 \|H(s)\|^2$. So

$$P_{out} = \|v_{S1}(s)\|^2 \frac{\|H(s)\|^2}{2 R_e} = \frac{\pi^2 V_g^2}{8R} \|H(s)\|^2 \quad (2-22)$$

Hence, the converter efficiency is:

$$\eta = \frac{P_{out}}{P_{in}} = \frac{\|H(s)\|^2}{R_e \cdot \text{Real}(Y_i(s))} \quad (2-23)$$

This expression models the losses associated with the tank network in a simple, circuit-oriented way. Tank network efficiency can be estimated by computing the tank transfer function $H(s)$ and the tank input admittance $Y_i(s)$, and then evaluating Eq. (2-23). An example is given in the following section, in which the influence of tank inductor core loss and capacitor esr on converter efficiency is determined.

2.2. Series Resonant Converter Example

The series resonant converter with switching frequency control is shown in Fig. 2.1. For this circuit, the tank network consists of a series L-C circuit, and Fig. 2.11 can be redrawn as in Fig. 2.12.

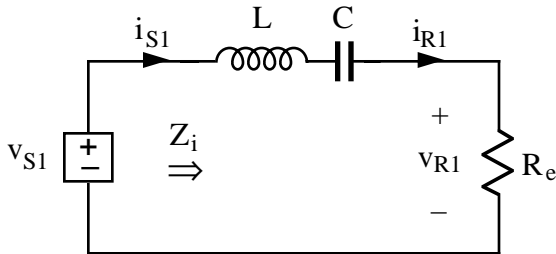


Fig. 2.12. Equivalent circuit which models the fundamental components of the tank waveforms in the series resonant converter.

The transfer function $H(s)$ is therefore:

$$\begin{aligned} H(s) &= \frac{R_e}{Z_i(s)} = \frac{R_e}{R_e + sL + \frac{1}{sC}} \\ &= \frac{\left(\frac{s}{Q_e \omega_0}\right)}{1 + \left(\frac{s}{Q_e \omega_0}\right) + \left(\frac{s}{\omega_0}\right)^2} \end{aligned} \quad (2-24)$$

where $\omega_0 = \frac{1}{\sqrt{LC}} = 2\pi f_0$
 $R_0 = \sqrt{\frac{L}{C}}$
 $Q_e = R_0/R_e$

The magnitude of $H(j2\pi f_s)$, which coincides with the converter dc conversion ratio $M = V/V_g$, is

$$M = \|H(j2\pi f_s)\| = \frac{1}{\sqrt{1 + Q_e^2 \left(\frac{1}{F} - F\right)^2}} \quad (2-25)$$

where $F = f_s / f_0$

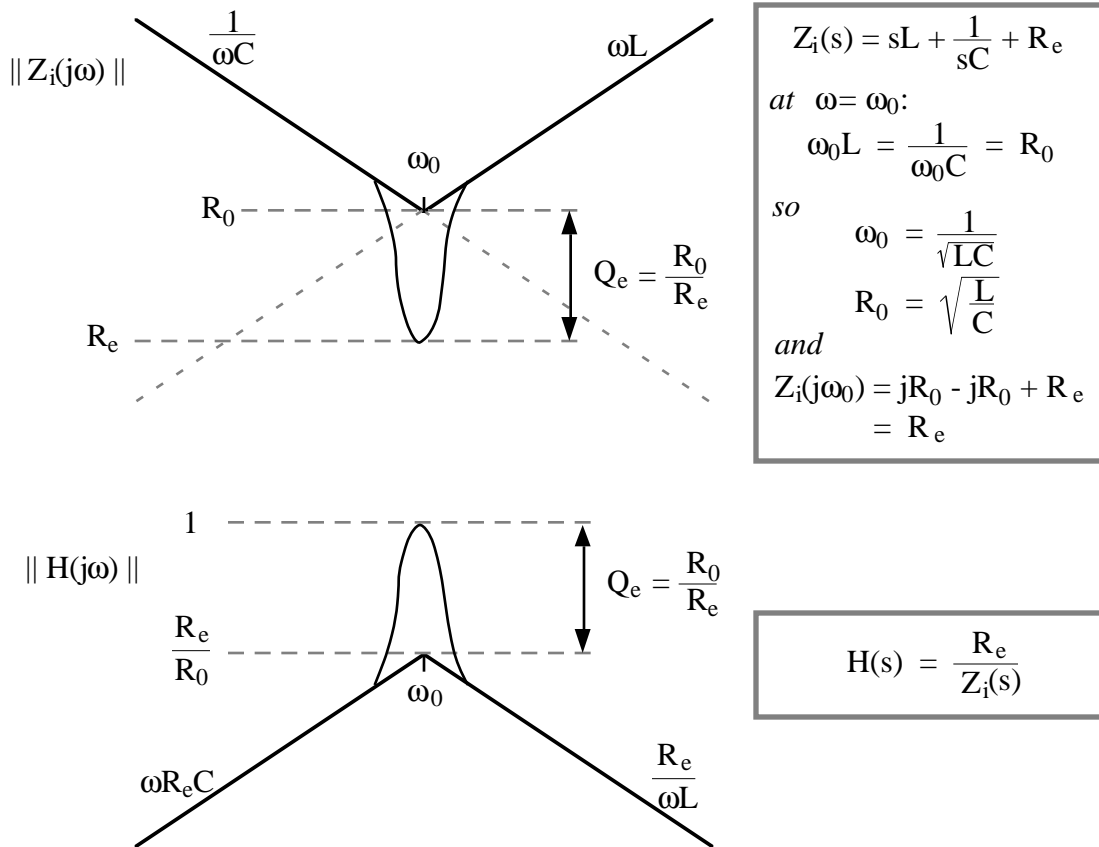


Fig. 2.13. Construction of the Bode diagrams of $Z_i(s)$ and $H(s)$ for the series resonant converter.

The Bode diagrams of $Z_i(s)$ and $H(s)$ are constructed in Fig. 2.13. Equation (2-25) is plotted in Figs. 2.14 and 2.15 for various values of Q_e and of switching frequency, and the approximate results are compared with the exact results of chapter 3. It can be seen that the dc conversion ratio is unity when the converter is excited at resonance, regardless of load. This is true because the series L-C circuit behaves as a short circuit at resonance: the impedances of the

tank inductor and capacitor are equal in magnitude but opposite in phase, and their sum is zero. The voltages v_S and v_R are therefore the same. It can also be seen that a decrease in the load resistance R , which increases the effective quality factor Q_e , causes a more peaked response in the vicinity of resonance.

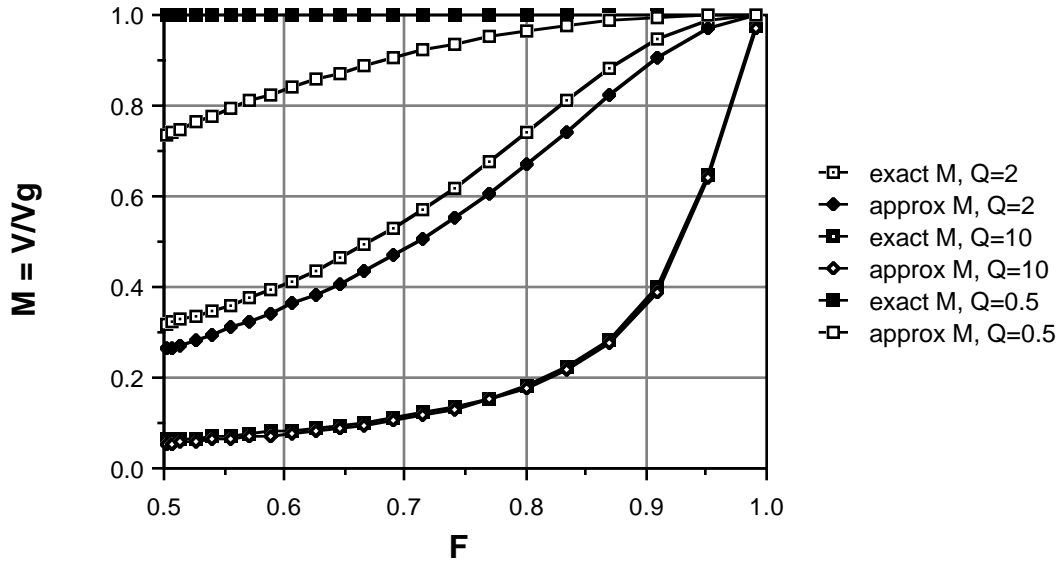


Fig. 2.14. Comparison of exact and approximate series resonant converter characteristics, below resonance.

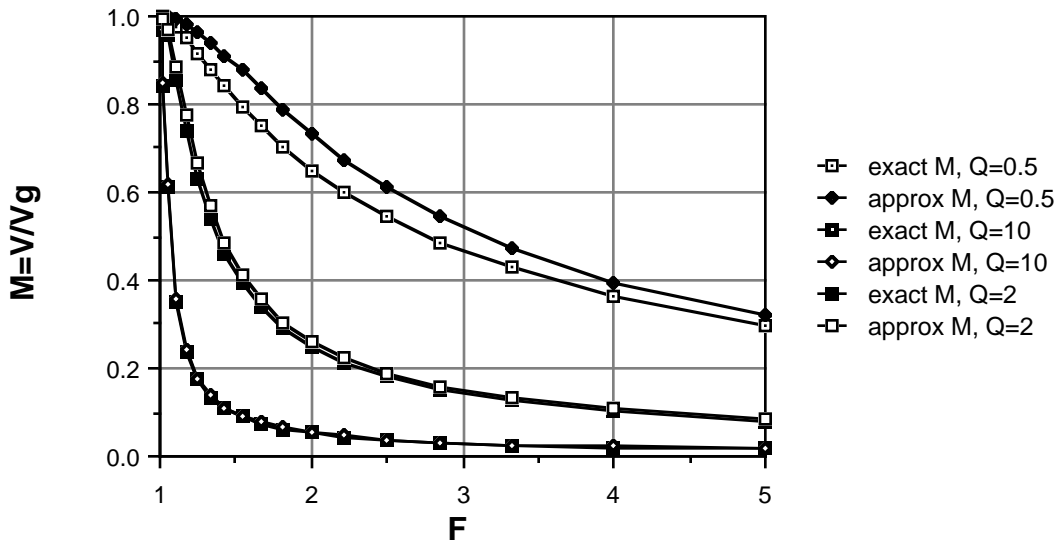


Fig. 2.15. Comparison of approximate and exact series resonant converter characteristics, above resonance.

Over what range of switching frequencies is Eq. (2-25) accurate? The response of the tank to the fundamental component of $v_S(t)$ must be sufficiently greater than the response to the

harmonics of $v_S(t)$. This is certainly true for operation above resonance because $H(s)$ contains a bandpass characteristic which decreases with a single pole slope for $f_S > f_0$. For the same reason, Eq. (2-25) is valid when the switching frequency is below but near resonance.

However, for switching frequencies f_S much less than the resonant frequency f_0 , the sinusoidal approximation breaks down completely because the tank responds more strongly to the harmonics of $v_S(t)$ than to its fundamental. For example, at $f_S = f_0/3$, the third harmonic of $v_S(t)$ is equal to f_0 and directly excites the tank resonance. Some other type of analysis must be used to understand what happens at these lower frequencies. Also, in the low-Q case, the approximation is less accurate because the filter response is less peaked, and hence does not favor the fundamental component as strongly. As shown in a later chapter, discontinuous conduction modes may then occur whose waveforms are highly non sinusoidal.

Efficiency

A similar analysis can be used to compute the converter efficiency. Let us model the effects of tank inductor core loss by a resistance R_P , and tank inductor winding resistance and tank capacitor equivalent series resistance (esr) by an effective resistance R_S , as shown in Fig. 2.16.

Standard circuit analysis can be used to show that the tank transfer function $H(s)$ is given by

$$H(s) = \frac{\left(\frac{s}{\omega_e}\right)\left(1 + \frac{s}{\omega_p}\right)}{1 + \left(\frac{s}{Q_e\omega_0}\right) + \left(\frac{s}{\omega_0}\right)^2} \quad (2-26)$$

where

$$\omega_0 = \frac{1}{\sqrt{LC} \frac{R_P + R_S + R_e}{R_P}}$$

$$\omega_e = \frac{1}{R_e C}$$

$$\omega_p = \frac{R_P}{L}$$

$$\frac{1}{Q_e} = \frac{R_0}{R_P} + \frac{R_e + R_S}{R_0}$$

$$R_0 = \sqrt{\frac{L}{C}} \cdot \sqrt{1 + \frac{R_S + R_e}{R_P}}$$

The efficiency is found by evaluation of Eq. (2-23). For the circuit of Fig. 2.16, the efficiency is:

$$\eta = \left(\frac{R_e}{R_S + R_e}\right) \frac{\left(1 + \frac{(2\pi L)^2}{R_P} f_S^2\right)}{\left(1 + \frac{(2\pi L)^2}{R_P (R_P \parallel (R_S + R_e))} f_S^2\right)} \quad (2-27)$$

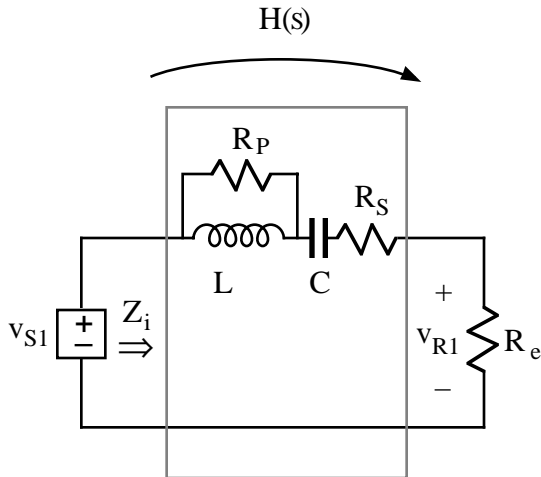


Fig. 2.16 Equivalent circuit used to model tank component losses.

A sketch of tank network efficiency vs. switching frequency is given in Fig. 2.17. To the extent that the sinusoidal approximation is valid, the efficiency at low frequency is asymptotic to the value $R_e / (R_S + R_e)$. The tank esr R_S is effectively in series with the load, and leads to a power loss in direct proportion to the load current. Hence, to obtain high efficiency, one should choose $R_S \ll R_e$.

As the switching frequency is increased, the inductor core loss begins to degrade the efficiency. This occurs when the denominator of Eq. (2-27) begins to increase. To avoid this, the switching frequency should be restricted to

$$f_S \ll \frac{1}{2\pi L} \sqrt{R_P (R_P \parallel (R_S + R_e))} \quad (2-28)$$

Alternatively, given a maximum desired switching frequency, Eq. (2-28) can be used to determine a lower bound on R_P .

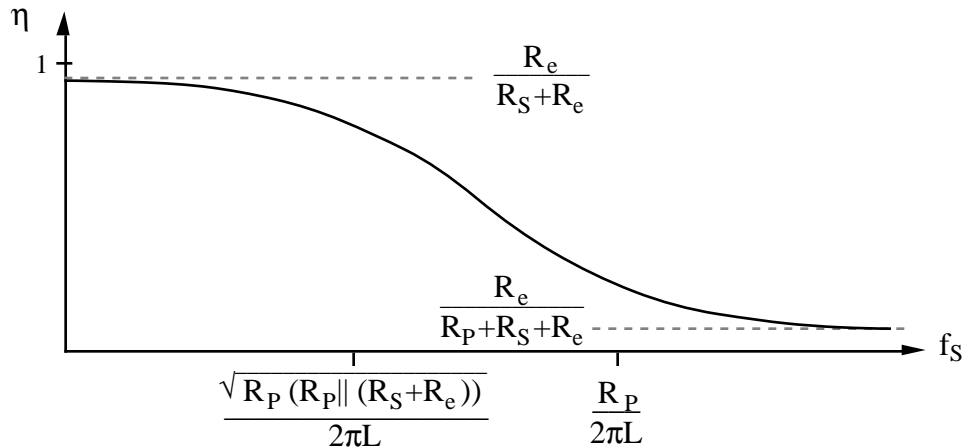


Fig. 2.17. Tank network efficiency vs. switching frequency.

Thus, sinusoidal approximations give an effective means of estimating the losses and efficiency degradations which arise owing to tank component nonidealities.

2.3. Subharmonic Modes of the Series Resonant Converter

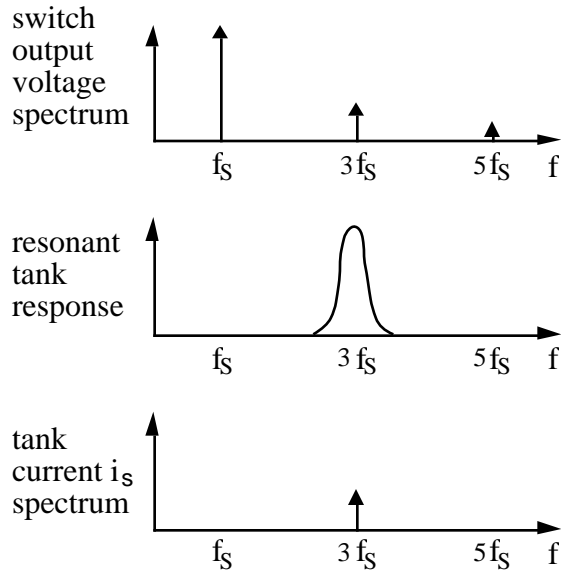


Fig 2.18 When the tank responds primarily to the third harmonic of the switching frequency, then frequency components other than the third harmonic may be neglected.

If the n^{th} harmonic of the switch output waveform $v_S(t)$ is close to the resonant tank frequency, $nf_S \sim f_0$, and if the tank effective quality factor Q_e is sufficiently large, then as shown in Fig. 2.18, the tank responds primarily to harmonic n . All other components of the tank waveforms can then be neglected, and it is a good approximation to replace $v_S(t)$ with its n^{th} harmonic component:

$$v_S(t) \cong v_{S_n}(t) = \frac{4 V_g}{n\pi T_S} \sin(n\omega_S t) \quad (2-29)$$

This differs from Eq. (2-2) because the amplitude is reduced by a factor of $1/n$, and the frequency is nf_S rather than f_S .

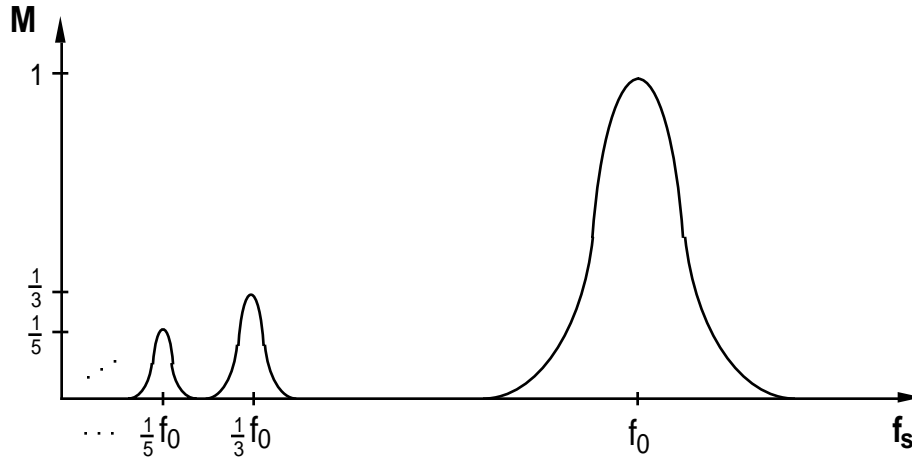


Fig. 2.19 The subharmonic modes of the series resonant converter. These modes occur when the harmonics of the switching frequency excite the tank resonance.

The arguments used to model the tank and rectifier/filter networks are unchanged from section 2.1. The rectifier presents an effective resistive load to the tank, of value $R_e = 8R/\pi^2$. In consequence, the converter dc conversion ratio is given by

$$M = \frac{V}{V_g} = \frac{\|H(j2\pi n f_s)\|}{n} \quad (2-30)$$

This is a good approximation provided that $n f_s$ is close to f_0 , i.e.,

$$(n-1) f_s < f_0 < (n+1) f_s \quad (2-31)$$

and Q_e is sufficiently large. Typical characteristics are plotted in Fig. 2.19.

The series resonant converter is not generally designed to operate in a subharmonic mode, since the fundamental modes yield greater output voltage and power, and hence higher efficiency. Nonetheless, the system designer should be aware of their existence, because inadvertent operation in these modes can lead to large signal instabilities.

2.4. The Parallel Resonant Converter

The parallel resonant converter is diagrammed in Fig. 2.20. It differs from the series resonant converter in two ways. First, the tank capacitor appears in parallel with the rectifier network rather than in series: this causes the tank transfer function $H(s)$ to have a different form. Second, the rectifier drives an inductive-input low-pass filter. In consequence, the value of the effective resistance R_e differs from that of the rectifier with a capacitive filter. Nonetheless, sinusoidal approximations can be used to understand the operation of the parallel resonant converter.

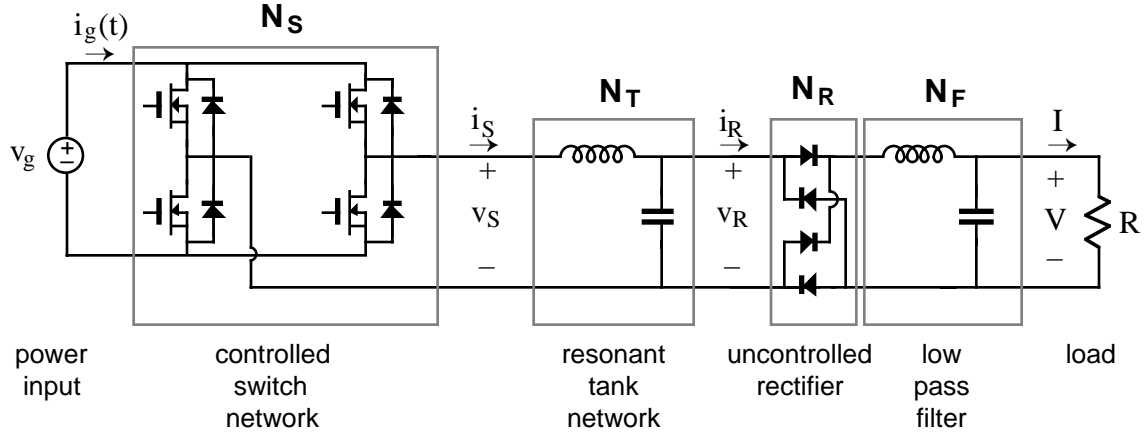


Fig. 2.20. Block diagram of the parallel resonant converter.

As in the series resonant converter, the switch network is controlled to produce a square wave $v_s(t)$. If the tank network responds primarily to the fundamental component of $v_s(t)$, then arguments identical to those of section 2.1 can be used to model the output fundamental components and input dc components of the switch waveforms. The resulting equivalent circuit is identical to Fig. 2.6.

The uncontrolled rectifier with inductive filter network can be described using the dual of the arguments of Section 2.1. In the parallel resonant converter, the output rectifiers are driven by the (nearly sinusoidal) tank capacitor voltage $v_R(t)$, and the diode rectifiers switch when $v_R(t)$ passes through zero as in Fig. 2.21. The rectifier input current $i_R(t)$ is therefore a square wave of amplitude I , and it is in phase with the tank capacitor voltage $v_R(t)$.

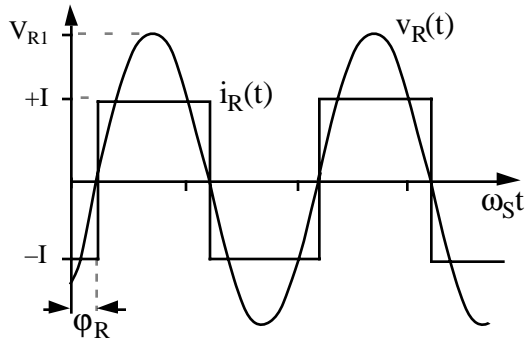


Fig. 2.21. Parallel resonant converter waveforms $v_R(t)$ and $i_R(t)$.

The output voltage V is equal to the dc component of $|v_R(t)|$:

$$V = \frac{2}{T_S} \int_0^{\frac{T_S}{2}} V_{R1} |\sin(2\pi f_{st} - \phi_R)| dt \quad (2-34)$$

So the load voltage V and the tank capacitor voltage amplitude are directly related in steady state.

Substitution of Eq. (2-27) and resistive load characteristics $V = IR$ into Eq. (2-26) yields:

$$R_e = \frac{\pi^2}{8} R = 1.2337 R \quad (2-35)$$

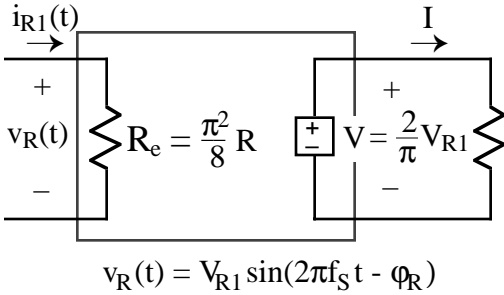


Fig. 2.22. An equivalent circuit for the rectifier with inductive output filter, which models the fundamental component of the ac side voltage, and the dc component of the dc side voltage, in the parallel resonant converter.

An equivalent circuit for the uncontrolled rectifier with inductive filter network is given in Fig. 2.22. This model is similar to the one used for the series resonant converter, Fig. 2.9, except that the roles of the rectifier input voltage v_R and current i_R are interchanged, and the effective resistance R_e has a different value. The model for the complete converter is given in Fig. 2.23.

Solution of Fig. 2.23 yields the converter dc conversion ratio:

$$M = \frac{V}{V_g} = \frac{8}{\pi^2} \| H(s) \|_{s=j2\pi f_s} \quad (2-36)$$

where $H(s)$ is the tank transfer function

$$H(s) = \frac{Z_0(s)}{sL} \quad (2-37)$$

and

$$Z_0(s) = sL \| \frac{1}{sC} \| R_e \quad (2-38)$$

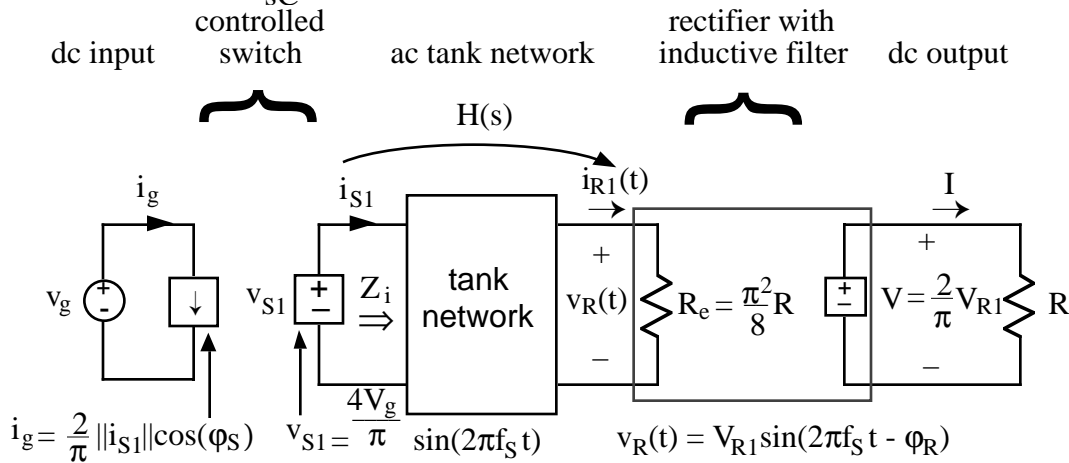


Fig. 2.23. Equivalent circuit for the parallel resonant converter, which models the fundamental components of the tank waveforms, and the dc components of the input current and output voltage.

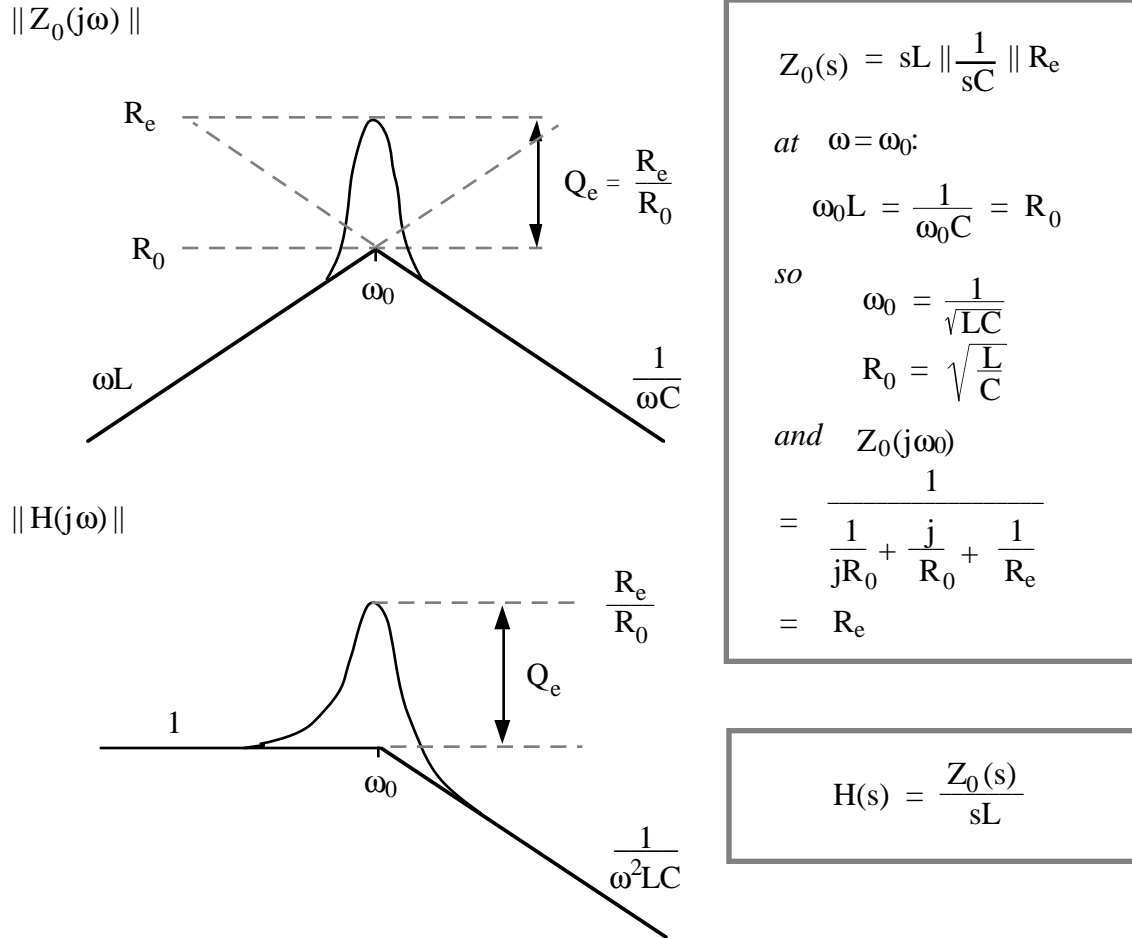


Fig. 2.24. Construction of Bode diagrams of $Z_i(s)$ and $H(s)$ for the parallel resonant converter.

The Bode magnitude diagrams of $H(s)$ and $Z_0(s)$ are constructed in Fig. 2.24. $Z_0(s)$ is the parallel combination of the impedance of the tank inductor L , capacitor C , and effective load R_e . The magnitude asymptote of the parallel combination of these components, at a given frequency, is equal to the smallest of the individual asymptotes ωL , $1/\omega C$, and R_e . Hence, at low frequency where the inductor impedance dominates the parallel combination, $\|Z_0(s)\| \cong \omega L$, while at high frequency the capacitor dominates and $\|Z_0(s)\| \cong 1/\omega C$. At resonance, the impedances of the inductor and capacitor are equal in magnitude but opposite in phase, so that their effects cancel. $\|Z_0\|$ is then equal to R_e :

$$\|Z_0(s)\|_{s=j\omega_0} = \frac{1}{\frac{1}{j\omega_0 L} + j\omega_0 C + \frac{1}{R_e}} = R_e \quad (2-39)$$

where $\omega_0 L = \frac{1}{\omega_0 C} = R_0$

The dc conversion ratio is therefore

$$\begin{aligned}
 M &= \frac{8}{\pi^2} \left\| \frac{1}{1 + \frac{s}{Q_e \omega_0} + \left(\frac{s}{\omega_0}\right)^2} \right\|_{s=j2\pi f_s} \\
 &= \frac{8}{\pi^2} \cdot \frac{1}{\sqrt{(1 - F^2)^2 + \left(\frac{F}{Q_e}\right)^2}}
 \end{aligned} \tag{2-40}$$

Equation (2-40) is compared with the exact converter solution in Fig. 2.25.

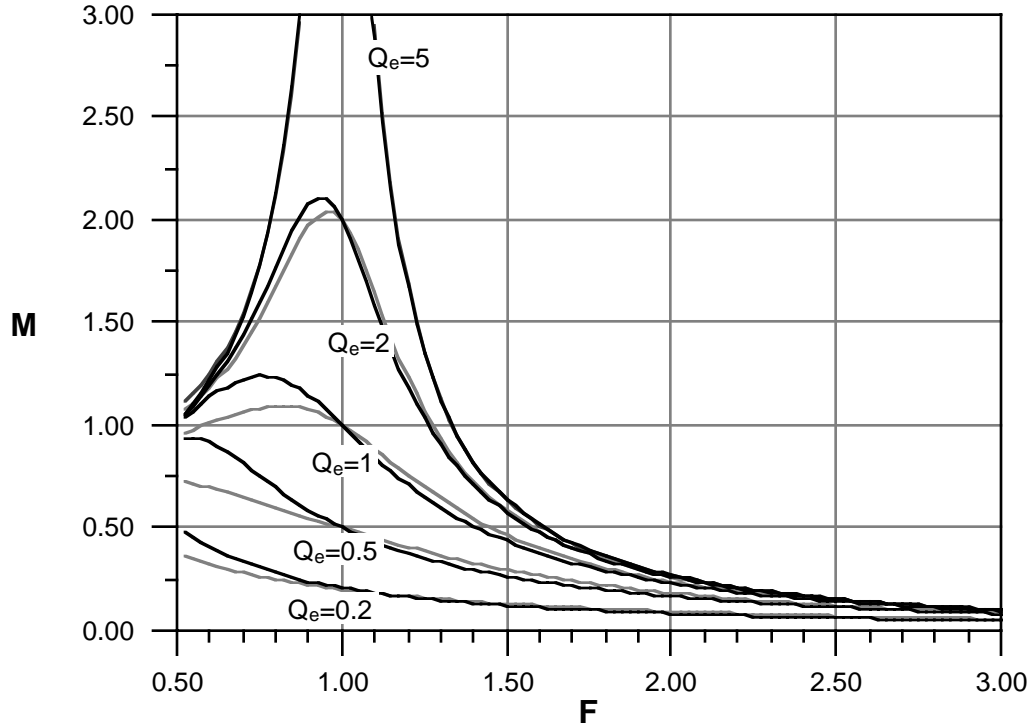


Fig. 2.25. Comparison of exact parallel resonant converter characteristics (solid lines) vs. the approximate solution, Eq. (2-40) (shaded lines).

2.5. Switching at Zero Current or Zero Voltage

Operation of the Full Bridge Below Resonance

An advantage of resonant converters is their reduced switching loss. When the series resonant converter is operated below resonance, a phenomenon known as “zero current switching” can occur, in which the transistors naturally switch off at zero current. With a simple circuit modification, the transistor turn-on transition can also be caused to occur at zero current. Let us consider the operation of the full bridge switch in more detail.

A full bridge circuit, realized using power MOSFET's and antiparallel diodes, is shown in Fig. 2.26. The switch output voltage $v_S(t)$, and its fundamental component $v_{S1}(t)$, as well as the approximately sinusoidal tank current waveform $i_S(t)$, are plotted in Fig. 2.27. At frequencies less than the tank resonant frequency, the input impedance of the tank network $Z_i(s)$ is dominated by the tank capacitor impedance. Hence, the tank presents an effective capacitive load to the bridge, and switch current $i_S(t)$ leads the switch voltage fundamental component $v_{S1}(t)$, as shown in Fig. 2.27. In consequence, the zero crossing of the current waveform $i_S(t)$ occurs before the zero crossing of the voltage $v_S(t)$.

For the half cycle $0 \leq t \leq T_S/2$, $v_S = +V_g$. For $0 \leq t \leq t_\beta$, the current $i_S(t)$ is positive and transistors Q_1 and Q_4 conduct. Then the diodes D_1 and D_4 conduct when

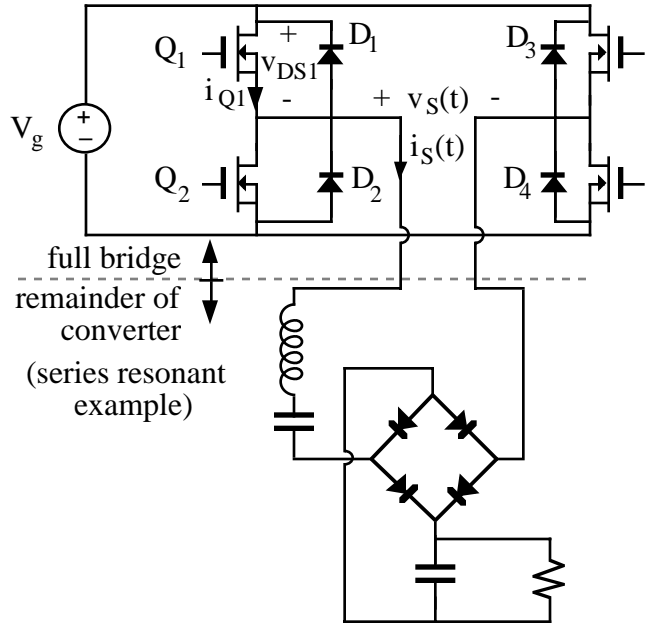


Fig. 2.26. Full bridge circuit implemented with power MOSFET's and antiparallel diodes in a series resonant converter circuit.

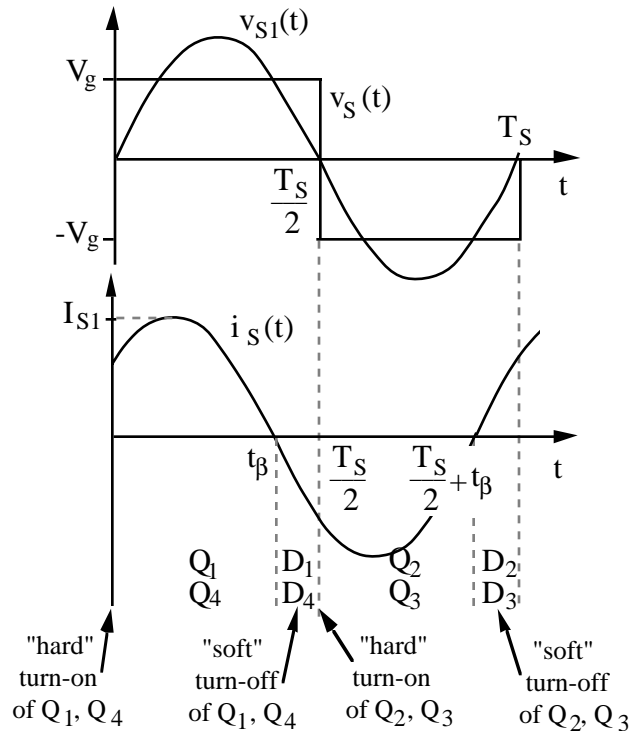


Fig. 2.27. Tank waveforms for the series resonant converter, operated below resonance. “Zero-current switching” aids the transistor turn off transitions.

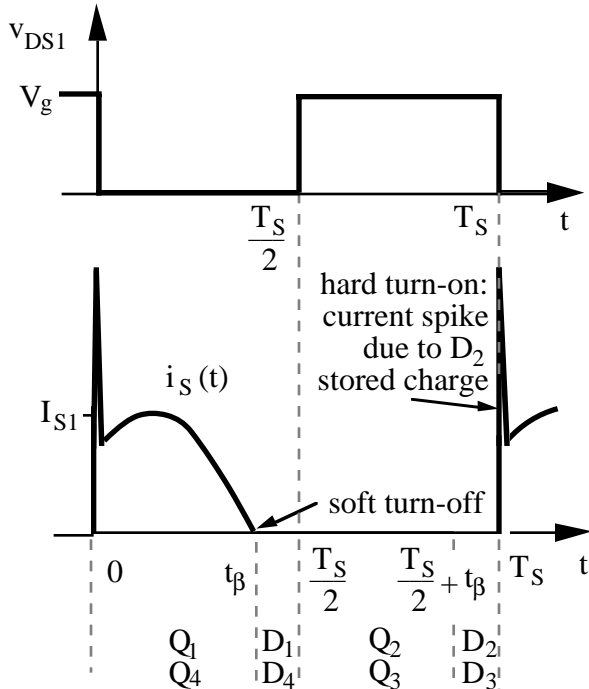


Fig. 2.28. Tank waveforms for the series resonant converter, operated below resonance. “Zero-current switching” aids the transistor turn off transitions.

$i_S(t)$ is negative, $t_\beta \leq t \leq T_S/2$. The situation during $T_S/2 \leq t \leq T_S$ is symmetrical. Since i_{S1} leads v_{S1} , the transistors conduct before their respective antiparallel diodes. Note that, at any given time during the D_1 conduction interval $t_\beta \leq t \leq T_S/2$, transistor Q_1 can be turned off without incurring switching loss. The circuit naturally causes the transistor turn off transition to be lossless, and long turn off switching times can be tolerated.

In general, “zero current switching” can occur when the resonant tank presents an effective capacitive load to the switches, and the switch current zero crossings occur before the switch voltage zero crossings. In the bridge configuration, zero current switching is characterized by the conduction sequence Q_1 - D_1 - Q_2 - D_2 , such that the transistors are turned

off while their respective antiparallel diodes conduct. It is possible, if desired, to replace the transistors with naturally-commutated thyristors whenever the zero-current-switching property occurs.

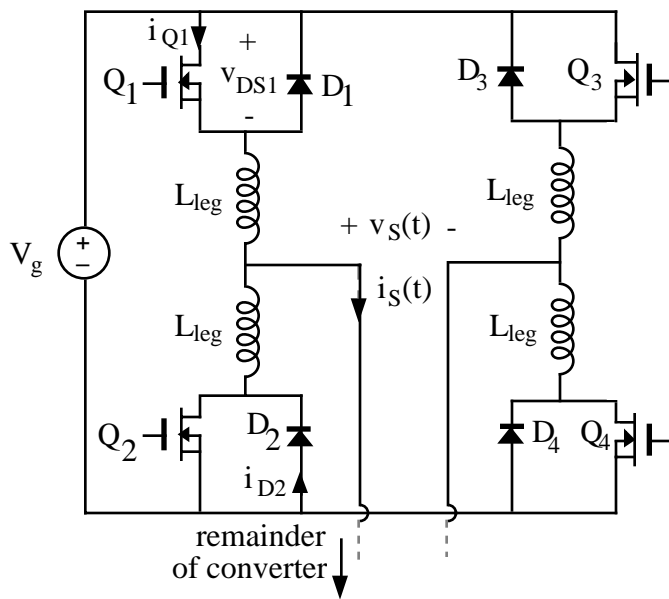


Fig. 2.29 Addition of small inductors L_{leg} , which effectively snub the transistor turn-on transition and reduce turn-on switching loss in the SRC operated below resonance.

The transistor turn on transition in Fig. 2.28 is similar to that of a PWM switch, and it is not lossless. During the turn on transition of Q_1 , diode D_2 must turn off. Neither the transistor current nor the transistor voltage is zero, Q_1 passes through a period of high instantaneous power dissipation, and switching loss occurs. As in the PWM case, the reverse recovery current of diode D_2 flows through Q_1 . This current spike can be the largest component of switching loss. In addition, the energy stored in the drain-to-source capacitances of Q_1 and Q_2

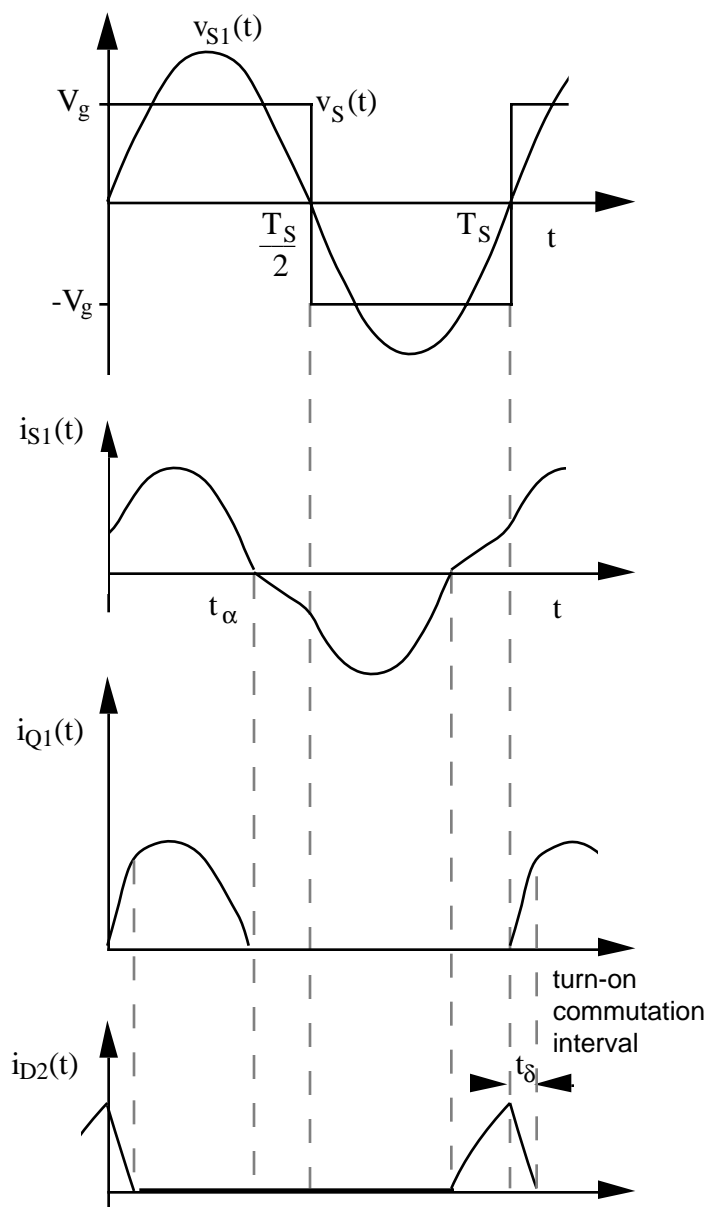


Fig. 2.30. Waveforms for the circuit of Fig. 2.29. During time t_δ the tank current commutes from D_2 to Q_1 .

and in the depletion layer capacitance of D_1 is lost when Q_1 turns on. To assist the transistor turn on process, small inductors are often introduced into the legs of the bridge (Fig. 2.29). During the normal Q_1 , D_1 , Q_2 , and D_2 conduction intervals, these inductors appear in series with the tank inductor L , and hence the effective total tank inductance is

$$L_{\text{effective}} = L + 2L_{\text{leg}} \quad (2-41)$$

In addition, these leg inductors introduce commutation intervals at transistor turn on. At the instant when Q_1 is turned on, the tank current flowing through diode D_2 begins to shift to Q_1 , at a rate determined by V_g and $2L_{\text{leg}}$. The transistor current magnitude is therefore limited by L_{leg} , rather than being determined by the stored charge in diode D_2 . During time t_δ ,

$$t_\delta = \frac{2 L_{\text{leg}} i_S(0)}{V_g} \quad (2-42)$$

where $i_S(0)$ is the tank current at the beginning of the commutation interval, the current in diode D_2 reaches zero, and D_2 turns off. The leg inductance L_{leg} is chosen such that t_δ is longer than the gate-driver-limited MOSFET turn-on time, but is much shorter than normal Q_1 , D_1 , Q_2 , and D_2 conduction intervals. Thus, the MOSFET is switched fully on before the drain current rises significantly above zero, and nearly lossless snubbing at turn-on occurs. This lossless snubbing of the diode D_2 stored charge during the Q_1 turn-on transition is probably the most common reason to use zero current switching.

A nonideality not considered in the discussion above is the effect of other semiconductor device capacitances. Transistor Q_1 output capacitance, diode D_1 junction capacitance, and diode D_1 stored charge can be modeled as effective parallel capacitances which are shorted out whenever

transistor Q_1 is turned on. In consequence, switching loss occurs equal to the total stored energy in these capacitances times the switching frequency. Similar switching losses occur in the other three legs of the bridge. This loss mechanism, while not as great as the loss owing to the stored charge in D_2 , can nonetheless be quite significant in converters operating from high input voltages and at high switching frequencies. It is often a significant disadvantage of zero current switching schemes.

Operation of the Full Bridge Above Resonance

When the series resonant converter is operated above resonance, a different phenomenon known as “zero voltage switching” can occur, in which the transistors naturally switch on at zero voltage. With a simple circuit modification, the transistor turn-off transition can also be caused to occur at zero voltage. Ideally, this process is the dual of the “zero current switching” process described in the previous section.

For the full bridge circuit of Fig. 2.26, the switch output voltage $v_S(t)$, and its fundamental component $v_{S1}(t)$, as well as the approximately sinusoidal tank current waveform $i_S(t)$, are plotted in Fig. 2.31. At frequencies greater than the tank resonant frequency, the input impedance of the tank network $Z_i(s)$ is dominated by the tank inductor impedance. Hence, the tank presents an effective inductive load to the bridge, and the switch current $i_S(t)$ lags the switch voltage fundamental component $v_{S1}(t)$, as shown in Fig. 2.31. In consequence, the zero crossing of the voltage waveform $v_S(t)$ occurs before the current waveform $i_S(t)$.

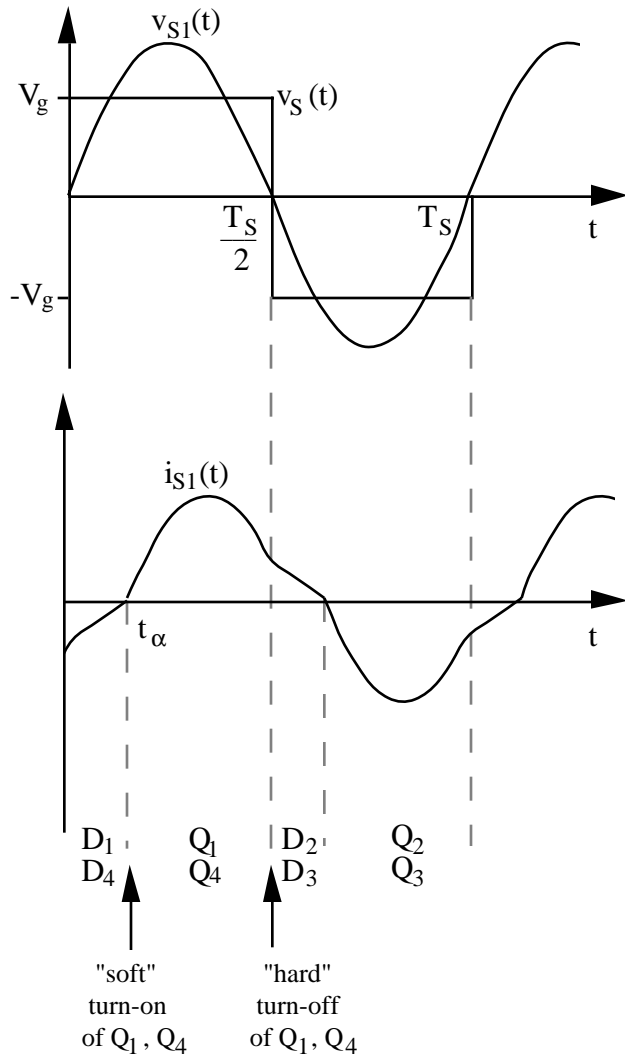


Fig. 2.31. Tank waveforms for the series resonant converter, operated above resonance. “Zero voltage switching” aids the transistor turn-on transitions.

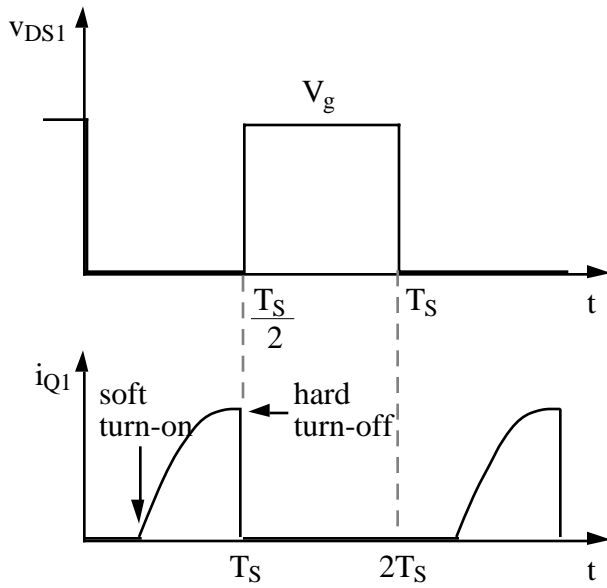


Fig. 2.32. Detail of Q_1 drain current and drain-source voltage waveforms, SRC example, operation above resonance.

For the half cycle $0 \leq t \leq T_S/2$, $v_S = +V_g$. For $0 \leq t \leq t_{\alpha}$, the current $i_S(t)$ is positive and the transistors Q_1 and Q_4 conduct, and the diodes D_1 and D_4 conduct when $i_S(t)$ is negative, $t_{\alpha} \leq t \leq T_S/2$. The situation during $T_S/2 \leq t \leq T_S$ is symmetrical. Since v_{S1} leads i_{S1} , the transistors conduct after their respective antiparallel diodes. Note that, at any given time during the D_1 conduction interval $0 \leq t \leq t_{\alpha}$, transistor Q_1 can be turned on without incurring switching loss. The circuit naturally causes the transistor turn-on transition to be lossless, and long turn-on switching times can be tolerated.

In general, “zero voltage switching” can occur when the resonant tank presents

an effective inductive load to the switches, and hence the switch voltage zero crossings occur before the switch current zero crossings. In the bridge configuration, zero voltage switching is characterized by the conduction sequence D_1 - Q_1 - D_2 - Q_2 , such that the transistors are turned on while their respective antiparallel diodes conduct. Since the transistor voltage is zero during the entire turn on transition, switching loss due to slow turn-on times or due to energy storage in any of the device capacitances does not occur at turn-on.

The transistor turn-off transition in Fig. 2.32 is similar to that of a PWM switch, and is not lossless. During the turn-off transition of Q_1 , diode D_2 must turn on. Neither the transistor current nor the transistor voltage is zero, Q_1 passes through a period of high instantaneous power dissipation, and switching loss occurs.

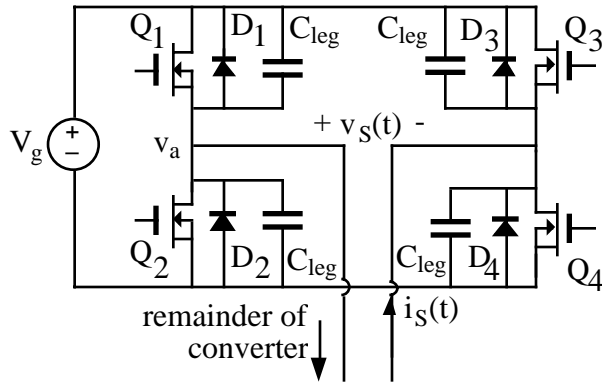


Fig. 2.33. Introduction of small capacitors C_{leg} , which effectively snub the transistor turn-off transition and can reduce turn-off switching loss in the SRC operated above resonance.

To assist the transistor turn off process, small capacitors may be introduced into the legs of the bridge, as demonstrated in Fig. 2.33. Alternatively, the existing device capacitances can be used. A delay is also introduced into the gate drive signals, so that there is a short commutation interval when all four transistors are off. During the normal Q_1 , D_1 , Q_2 , and D_2 conduction intervals, the leg capacitors appear

in parallel with the semiconductor switches, and have no effect on the converter operation. However, these capacitors introduce commutation intervals at transistor turn-off. When Q_1 is turned off, the tank current $i_L(T_S/2)$ flows through the switch capacitances C_{leg} instead of Q_1 , and the voltage across Q_1 and C_{leg} increases. Eventually, the voltage across Q_1 reaches V_g ; diode D_2 then becomes forward-biased. The length of this commutation interval is:

$$t_\delta = \frac{2 C_{leg} V_g}{i_L(T_S/2)} \quad (2-43)$$

where $i_L(T_S/2)$ is the tank current at the beginning of the commutation interval, the voltage reaches zero, and D_2 becomes forward-biased. The leg capacitance C_{leg} is chosen such that t_δ is longer than the gate-driver-limited MOSFET turn-off time, but is much shorter than normal Q_1 , D_1 , Q_2 , and D_2 conduction intervals. Thus, the MOSFET is switched fully off before the drain voltage rises significantly above zero, and nearly lossless snubbing at turn-off occurs. The fact that none of the semiconductor device capacitances or stored charges lead to switching loss is the major advantage of zero-voltage switching, and is the most common motivation for its use.

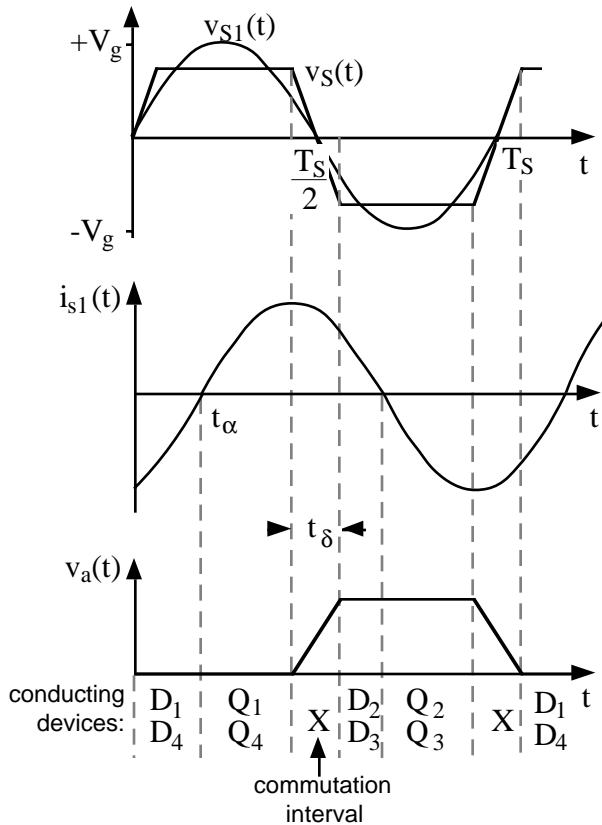


Fig. 2.34. Waveforms for the circuit of Fig. 2.33. During the commutation interval t_δ , all semiconductor devices are in the off state, and the tank circuit $i_S(t)$ charges or discharges the capacitors, C_{leg} .

An additional advantage is the reduction of EMI associated with device capacitances. In conventional PWM converters and, to a lesser extent, in zero-current switching converters, significant high frequency ringing and current spikes are generated by the rapid charging and discharging of the semiconductor device capacitances at turn on and/or turn off. Converters in which all semiconductor devices switch at zero voltage inherently do not generate this type of EMI.

A nonideality not considered in the discussion above is the effect of semiconductor package inductances. These inductances are open-circuited whenever the semiconductor device is turned off. In consequence, switching loss occurs equal to the total stored energy in these inductances times the switching frequency. This loss mechanism can be significant in converters operating with high currents and

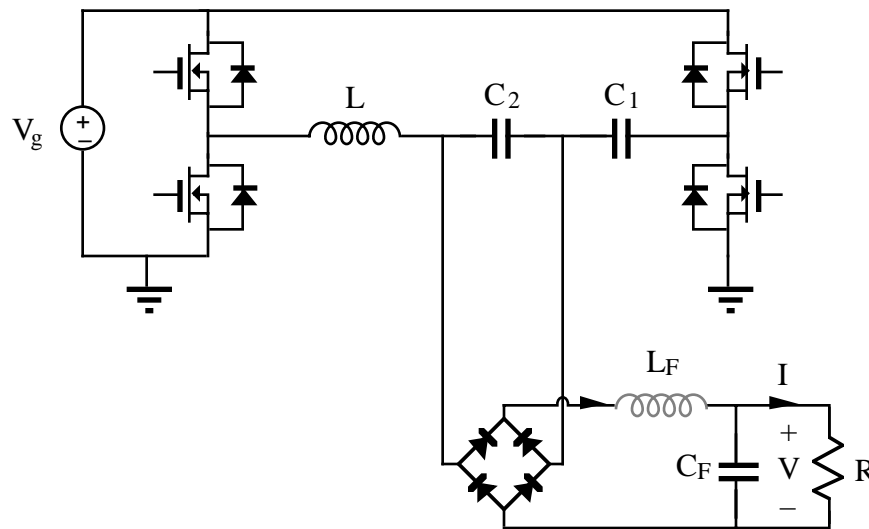
low input voltages and at high switching frequencies.

REFERENCES

- [1] R.L. Steigerwald, "A Comparison of Half-Bridge Resonant Converter Topologies," IEEE Applied Power Electronics Conference, 1987 Proceedings, pp. 135-144, March 1987.
- [2] R. Severns, "Topologies for Three Element Resonant Converters," IEEE Applied Power Electronics Conference, 1990 Proceedings, pp. 712-722, March 1990.

PROBLEMS

1. Analysis of the LCC converter



The "LCC" converter shown above contains both series and parallel tank capacitors.

- a) Using the sinusoidal approximation method, find an expression for the dc conversion ratio M of this converter.
- b) For large C_1 , the circuit becomes essentially a parallel resonant converter with added blocking capacitor C_1 . Use the approximate factorization method to approximate the tank transfer function $H(s)$ for this case. Show that your result of part (a) reduces to the parallel resonant converter M , with an added rolloff (inverted pole) for low switching frequencies due to C_1 . Identify a resonant frequency and Q for this case, and sketch typical curves of M vs. F for a few values of $Q > 1$.

- c) Use the approximate factorization method to approximate the tank transfer function $H(s)$ for large C_2 . For this case, the resonance occurs at approximately

$$f_0 = \frac{1}{2\pi\sqrt{LC_1}}$$

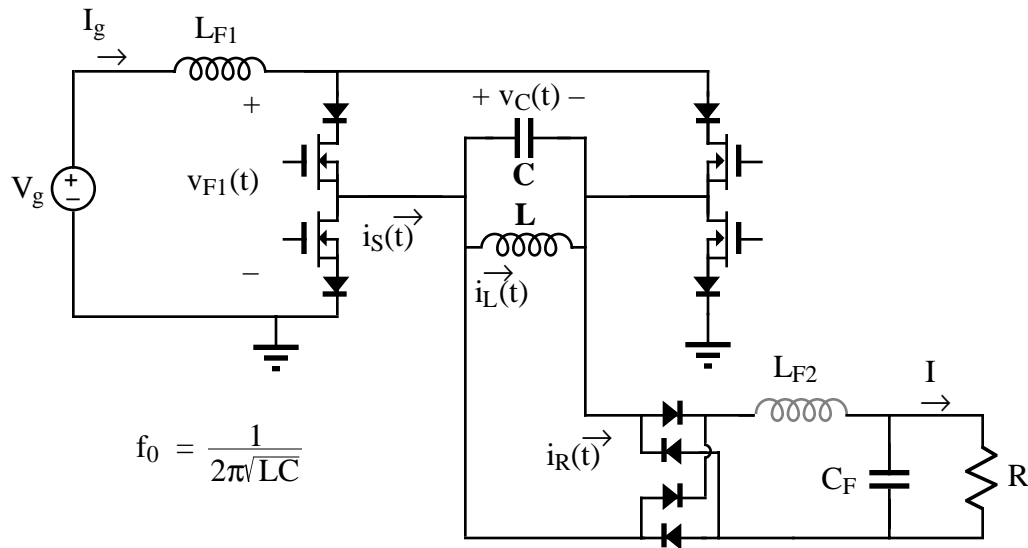
What is the Q ?

- d) For the case when $C_1 = C_2 = C$, sketch typical $\|H(s)\|$ asymptotes for the high Q case, i.e., $R_e \gg R_0$ where

$$R_0 = \sqrt{\frac{L}{2C}}$$

Identify salient features.

2. Dual of the series resonant converter



L_{F1} , L_{F2} , and C_F are large filter elements, whose switching ripples are small. L and C are tank elements, whose waveforms i_L and v_C are nearly sinusoidal.

- a) Using the sinusoidal approximation method, develop equivalent circuit models for the switch network, tank network, and rectifier network.
- b) Sketch a Bode diagram of the parallel LC parallel tank impedance.
- c) Solve your model. Find an analytical solution for the converter voltage conversion ratio $M = V/V_g$, as a function of the effective Q_c and the normalized switching frequency $F = f_s/f_0$. Sketch M vs. F .
- d) What can you say about the validity of the sinusoidal approximation for this converter? Which parts of your M vs. F plot of part (c) are valid and accurate?
- e) Below resonance, does the converter operate with zero-voltage switching or with zero-current switching? What about above resonance?